Contents lists available at ScienceDirect

Journal of Cleaner Production

journal homepage: www.elsevier.com/locate/jclepro

Microalgae biomass as a sustainable precursor to produce nitrogen-doped biochar for efficient removal of emerging pollutants from aqueous media

María González-Hourcade [a], Glaydson Simões dos Reis [a,*], Alejandro Grimm [a], Van Minh Dinh [b], Eder Claudio Lima [c], Sylvia H. Larsson [a], Francesco G. Gentili [a]

[a] Swedish University of Agricultural Sciences, Department of Forest Biomaterials and Technology, 90183, Umeå, Sweden
[b] Technical Chemistry, Department of Chemistry, Chemical-Biological Centre, Umeå University, SE-90187, Umeå, Sweden
[c] Institute of Chemistry, Federal University of Rio Grande do Sul (UFRGS), Av. Bento Gonçalves, 9500, Porto Alegre, RS, Brazil

ARTICLE INFO

ABSTRACT

Preparing sustainable and highly efficient biochars as adsorbents remains a challenge for organic pollutant management. Herein, a novel nitrogen-doped carbon material has been synthesized via a facile and sustainable single-step pyrolysis method using a wild mixture of microalgae as novel carbon precursor. Phosphoric acid (H_3PO_4) was employed as activation agent to generate pores in the carbon material. In addition, the effect of melamine (nitrogen source) was evaluated over the biochar properties by the N-doping process. The results showed that the biochar's specific surface area (SSA) increased from 324 to 433 m^2 g^{-1} with the N-doping process. The N-doping process increased the percentage of micropores in the biochar structure. Chemical characterization of the biochars indicated that the N-doping process helped to increase the graphitization process of the biochar and the contents of oxygen and nitrogen groups on the carbon surface. The biochars were successfully tested to adsorb acetaminophen and treat two synthetic effluents, and the N-doped biochar presented the highest efficiency. The kinetics and equilibrium data were well represented by the General-order model and the Liu isotherm model, respectively. The maximum sorption capacities attained were 101.4 and 120.7 mg g^{-1} for the non-doped and doped biochars, respectively. The acetaminophen adsorption mechanism suggests that the pore-filling was the dominant mechanism for acetaminophen uptake. The biochars could efficiently remove up to 74% of the contaminants in synthetic effluents.

1. Introduction

During the past 20 years, the presence of emerging contaminants (ECs) in water bodies has attracted massive attention from the scientific community due to their inherent capability to produce undesirable biological effects on living organisms and subsequent negative impacts on natural environments (Kroon et al., 2020). The main source of ECs in surface waters are chemical substances derived from human and industrial activities (Von der Ohe et al., 2011). The vast majority of ECs are not included in routine monitoring programs but can cause deleterious effects on living beings even at trace concentrations (Daughton, 2014).

Analgesic medicines for pain relief are among the most extensively consumed chemicals classified as ECs (Klotz, 2012). These types of drugs are highly soluble in water and are not completely metabolized in the human body (Boumya et al., 2021), meaning that their use may lead to

significant damage to living organisms if contaminated waters are not treated properly (Klotz, 2012). It has been reported that ECs like acetaminophen at high concentrations ($>1.8\,\mu g/L$) would be toxic to aquatic organisms (Klotz, 2012). Therefore, developing methods for treating polluted water remains a challenge since conventional water and wastewater treatment plants (WTPs) are incapable of removing ECs (Daughton, 2014).

Advanced wastewater treatment technologies that are capable of removing ECs are based on biological treatments (Kanaujiya et al., 2019), micro-and nanofiltration (Dharupaneedi et al., 2019), and advanced oxidative processes (Fast et al., 2017). However, these treatments have serious drawbacks, such as high implementation costs and high by-product generation. According to the literature (Bădescu et al., 2018), methods based on adsorption appear to be a suitable, affordable, efficient, and straightforward way to remove ECs. This technology also has advantages, such as the possibility of regenerating the adsorbent,

meaning that the generation of by-products can be minimized to a greater extent.

Carbonaceous materials such as activated carbons and biochars are ones of the most efficient types of adsorbents for the removal of ECs from wastewaters due to their well-developed porosity, high specific surface area (SSA), and chemical surface functionalities (Dos Reis et al., 2021a). Biochar is one of the main products from the pyrolysis of biomass and is considered a valuable material that generally improves the economy of the process if used reasonably (Ko et al., 2004). These carbon materials are prepared through different thermochemical routes, and their properties can be tailored to obtain high-performance adsorbents for removing ECs from polluted waters (Dos Reis et al., 2021a). Research works have shown that the biochar can be modified in terms of its chemical structure and surface functionalities by heteroatom doping (e. g., nitrogen) to boost the adsorption properties (Lin et al., 2022). In addition, nitrogen is an electron donor group that lead to electron delocalization in the carbon structure, improving the material's conductivity (Lin et al., 2022), which in turn could boost the adsorption process by electrostatic interactions between ECs and the surface of the biochars (Xu et al., 2022).

Biomasses that are often used for the production of biochars are different types of plants such as agricultural wastes (Naeem et al., 2019), tree (Umpierres et al., 2018), fruit seeds (Kasperiski et al., 2018), sewage sludge (Dos Reis et al., 2016), marine and freshwater biomasses (Ilnicka and Lukaszewicz, 2018). The over-ground carbon precursors (agricultural and woody biomasses) are the predominant for producing biochars (Lewoyehu, 2021). During the last decades, fast-growing organisms such as microalgae have been used as an aid to remove nitrogen and phosphorus from municipal wastewater (Mohsenpour et al., 2021). The microalgae biomass generated during the process is usually separated from the water when the process is completed, which results in a by-product that needs to be disposed of. Due to the fast-growing rate of these organisms, this type of by-products from wastewater treatment plants would be an ideal precursor for the development of carbon-based adsorbents. All published research focused on the production of activated biochar from microalgae has been dedicated to studying axenic cultures of model microalgae species such as *Chlorella* ssp (Guo et al., 2021). and Nannochloropsis gladina (Masoumi and Dalai, 2020) among others. None of these works has evaluated the suitability of polycultures of microalgae cultivated directly on untreated municipal wastewater. This work focuses on the development and characterization of activated biochars produced from a wild mixture of microalgae obtained from a pilot-scale algal cultivation facility located in Umeå, northern Sweden (63°86' N), that uses these types of organisms to treat municipal sewage water (Lage et al., 2021).

Development of adsobents from a wild mixture of microalgae was carried out using H_3PO_4 as activation agent and melamine (nitrogen source) to produce novel microalgae-based nitrogen-doped biochar. The biochar was prepared under environmentally benign conditions using water in the leaching-out process instead of acid or basic solutions commonly used to remove by-products from the carbonaceous matrix (Thue et al., 2020). The sustainable design and the application of a wild mixture of microalgae as a substrate for developing this novel adsorbent promote the tenets of green chemistry.

The current state-of-the-art presents a large gap between our ability to produce different carbon materials from biomasses and how their properties are connected to the resulting carbon performances in adsorbing pollutants from waters or performances in other possible applications (Yaashikaa et al., 2020). This research helps diminish that gap by explicitly focusing on the minute correlation of carbon properties after the doping process and the resulting material properties. The surface and structure of the nitrogen-doped carbon materials can be modified, in terms of their chemical structure and surface functionalities, to create materials with improved performance regarding their target application. Therefore, this research can provide a reasonable understanding of the effect of the nitrogen-doped process on the carbon

physical-chemical and adsorption properties of the doped biochar.

The biochars were prepared at a pyrolysis temperature of 600 °C. The effects of the doping process were evaluated according to the biochar's physicochemical and adsorption properties. The biochars were fully characterized in terms of their textural properties by N_2 adsorption-desorption isotherms and scanning electron microscopy (SEM), and surface functionalities were identified using Raman spectroscopy, X-ray photoelectron (XPS) spectroscopy, and Fourier transformed infrared (FT-IR). The ability of the biochars to remove ECs from water was tested using acetaminophen as a model contaminant. The effect of adsorbent mass and pH, kinetic and equilibrium studies, and efficiency for treatment of synthetic effluents were evaluated.

2. Materials and methods

2.1. Microalgae material, reagents and chemicals

A polyculture of microalgae was used as raw material for biochar synthesis. The microalgae were cultivated in a raceway pond located in Umeå, northern Sweden (63° 86' N) at Umeå Energy (Umeå, Sweden) combined heat and power plant (CHP-plant). The pond was10 m long, 2 m wide and aproximatelly 0.3 m deep which gives a surface area of 20 m^2 and a volume of 6 m^3. The raceway pond received municipal untreated wastewater influent collected from a local wastewater treatment plant. The algae were grown under a batch regime for 6 days (The growth curve was not measured). Microalgae biomass was harvested once a week by sedimentation followed by continuous centrifugation at $3949 \times g$ with a flow of approx. 1L/min (US Filtermaxx, Jacksonville, Florida, USA). Immediately after harvest, the algal biomass was frozen, then dried at 105 °C in an oven for 28 h and milled using a Cyclotec (FOSS Nordic A/S, Hilleroed, Denmark). More detailed information about process conditions can be found elsewhere (Lage et al., 2021). The polyculture of the wild algae population mainly includes the following microalgae strains *Coelastrum* ssp., *Desmodesmus* ssp., *Scenedesmus* ssp., and *Chlorella* ssp., whose composition is 22.0% carbohydrate, 27.9% protein, 21.0% lipid, 14.1% ash.

Deionized water was used during the entire investigation. All reagents and chemicals were of analytical grade purchased from Sigma-Aldrich (Merck KGaA, Germany) and used as such. The purity of the chemicals were 85 wt% (H_3PO_4) water solution, 99% (melamine) and >99% (acetaminophen). The phosphoric acid was diluted with dionised water to a concentration of 50 wt% and used for the preparation of the activated biochars.

2.2. Impregnation and activation process

Algae precursor (20 g) was mixed with phosphoric acid (50 wt %) using a weight ratio of precursor: acid of 1:3 to obtain a homogeneous paste (Dos Reis et al., 2021b). Precursor samples were doped with melamine (nitrogen source) using a weight ratio of 1: 3: 0.1 for algae, acid, and melamine. The activation process was carried out in one step by pyrolysis in an inert atmosphere using a tubular stainless steel reactor (diameter of 100 mm and length of 200 mm) equipped with a thermocouple to measure the temperature of the sample. The impregnated precursor was placed in the reactor and heated from room temperature to a final temperature of 600 °C by the aid of a muffle furnace (Carbolite Gero Elf 11/23 chamber furnace, Neuhausen Germany). Pyrolysis was carried out under N_2 gas flow (500 ml/min, 99.99%) at a heating rate of 10 °C/min. The final temperature was kept for 1 h; whereafter the sample was permitted to cool down to <150 °C under a nitrogen gas flow of 250 ml/min. After this, the N_2 gas was closed, and the sample cooled down to room temperature. Removal of by-products from the carbonaceous matrix was performed by washing the produced biochars several times successively with hot water (100 °C) until the washing waters attained the pH of deionized water (pH 6.0). Finally, the biochar samples were dried overnight at 100 °C. The biochars were named

Biochar-600 (biochar pyrolyzed at 600 °C without nitrogen doping) and Doped-biochar-600 (biochar pyrolyzed at 600 °C with nitrogen doping).

2.3. Characterization of microalgal-derived biochars

N₂ adsorption/desorption isotherm analysis (Tristar 3000 apparatus, Micrometrics Instrument Corp., Norcross, GA, USA) was performed to quantify the porosity (by DFT method) and surface area (BET method). Before the analysis, the biochars were degassed at 180 °C for 3 h in an N₂ atmosphere. The specific surface area was calculated in the relative pressure interval of 0.05–0.3 using the Brunauer–Emmett–Teller (BET) method (Dos Reis et al., 2021a). Mesopore size and distribution were calculated using the Barrett–Joyner–Halenda (BJH) method from desorption curves, while the micropore area values were calculated using the t-plot method (Dos Reis et al., 2021b).

The morphology of microalgal biochars was examined by Scanning Electron Microscopy (SEM) using a Carl Zeiss Merlin instrument (FESEM, ZEISS Sigma HD, Jena, Germany) equipped with an in-lens secondary electron detector. The instrument was operated at an accelerating voltage of 5 kV and probe current of 100 pA. Samples were attached to carbon tape mounted on aluminum stubs and coated with 2 nm platinum using a Quorum Technologies Q150T ES device.

Raman spectra were collected using a Bruker Bravo spectrometer (Bruker, Ettlingen, Germany) attached to a docking measuring station. Shortly, 0.5 g of AC samples were manually ground using an agate mortar and pestle, placed in 2.5-mL glass vials, and scanned in the 300–3200 cm⁻¹ spectral range at 4 cm⁻¹ resolution for 256 scans. Min–Max normalization over the 1000–2000 cm⁻¹ region and smoothing (9 points) was done using the built-in functions of the OPUS software (version 7, Bruker Optik GmbH, Ettlingen, Germany). No baseline correction was needed.

XPS spectra were collected using a Kratos Axis Ultra DLD electron spectrometer (Shizuoka, Japan) using a monochromated Al Kα source operated at 150 W. An analyzer pass energy of 160 eV for acquiring survey spectra and a pass energy of 20 eV for individual photoelectron lines were used. Because activated carbon is conductive, no charge neutralization system was used. The binding energy (BE) scale was calibrated following the ASTM E2108 and ISO 15,472 standards. Processing of the spectra was accomplished with the Kratos software.

The nitrogen content was determined using an elemental analyzer (EA-IsoLink, Thermo Fisher Scientific, Bremen, Germany). Shortly, 0.05 g oven-dried samples were used to determine the total nitrogen (N) content in the biochars.

2.4. Batch adsorption

Different concentrations of acetaminophen were used for the adsorption tests that varied from 30 to 1000 mg L⁻¹. The pH effect on the acetaminophen removal was also studied, and the experiments were performed at pHs from 2.0 to 10.0. Acetaminophen solution amounts of 20 mL were inserted in 50.0 mL plastic tubes containing different biochar masses varying from 20 to 100 mg to study the effect of the adsorbent mass on the sorption capacity. All the adsorption tests were performed at a fixed temperature of 23 °C. The kinetics was studied by agitating the tubes containing the adsorbent in a shaker at contact times varying from 1 to 360 min. Afterward, the biochars were separated from the solutions by a centrifugation process, and with a pipette, suitable amounts of solution were withdrawn to measure the residual acetaminophen concentration using ultraviolet spectrophotometry (Shimadzu 1800) at a maximum wavelength of 244 nm. The adsorption capacity (Equation (1)) and the percentage of acetaminophen removed (Equation (2)) are given below:

$$q = \frac{(C_0 - C_f)}{m}.V \tag{1}$$

$$\% \ Removal = 100.\frac{(C_0 - C_f)}{C_0} \tag{2}$$

where m is the biochar masses (g); C_o and C_f are the initial and final acetaminophen concentrations (mg L⁻¹), respectively; q is the adsorption capacity of acetaminophen uptaken by the biochars (mg g⁻¹), and V is the volume of acetaminophen solution (L).

2.5. Adsorption kinetics and equilibrium models

The kinetic data were fitted using the pseudo-first-order, pseudo-second-order, and general-order models (Lima et al., 2019). The equations of these respective models are shown in Equations (3)–(5).

$$q_t = q_e.[1 - \exp(-k_1.t)] \tag{3}$$

$$q_t = \frac{k_2.q_e^2.t}{1 + q_e.k_2.t} \tag{4}$$

$$q_t = \left(q_e - \frac{q_e}{\left[k_N.(q_e)^{n-1}.t.(n-1) + 1 \right]^{1/(1-n)}} \right) \tag{5}$$

where t is the contact time (min); q_t, q_e are the sorption capacities at time t and the equilibrium, respectively (mg g⁻¹); k_1 is the pseudo-first-order rate constant (min⁻¹); k_2 is the pseudo-second-order rate constant (g mg⁻¹ min⁻¹); k_N is the General-order constant rate [min⁻¹.(g mg⁻¹)ⁿ⁻¹)], n is the dimensionless general-order exponent.

The equilibrium data were fitted using Langmuir, Freundlich, and Liu's models; equations (6)–(8) show the corresponding models (Lima et al., 2016).

$$q_e = \frac{Q_{max}.K_L.C_e}{1 + K_L.C_e} \tag{6}$$

$$q_e = K_F.C_e^{1/nF} \tag{7}$$

$$q_e = \frac{Q_{max}.(K_g.C_e)^{nL}}{1 + (K_g.C_e)^{nL}} \tag{8}$$

where q_e is sorption capacity at equilibrium (mg g⁻¹); C_e is the adsorbate concentration at equilibrium (mg L⁻¹); Q_{max} is the maximum sorption capacity of the adsorbent (mg g⁻¹); K_L is the Langmuir equilibrium constant (L mg⁻¹); K_F is the Freundlich equilibrium constant [mg.g⁻¹. (mg.L⁻¹)⁻¹/ⁿF]; K_g is the Liu equilibrium constant (L mg⁻¹); n_F and n_L are the dimensionless exponents of Freundlich and Liu model, respectively.

The quality control of adsorption data is further described elsewhere (Thue et al., 2020). Nonlinear fitting of kinetic and equilibrium data was performed using the Microcal Origin (2020) software (Thue et al., 2020). The nonlinear fitting was obtained using the Simplex method and the Levenberg–Marquardt algorithm for performing this task (Prola et al., 2013). The adequacy of the kinetic and equilibrium models was statistically assessed employing the adjusted determination coefficient (R2adj) and the standard deviation of residues (SD) (Dos Reis et al., 2021b) shown in equations (9) and (10) below.

$$R_{adj}^2 = 1 - (1 - R^2).\left(\frac{n-1}{n-p-1} \right) \tag{9}$$

$$SD = \sqrt{\left(\frac{1}{n-p} \right).\sum_i^n \left(q_{i,\ exp} - q_{i,\ model} \right)^2} \tag{10}$$

where $q_{i,\ model}$ is the individual model sorption capacity expected by the model; $q_{i,\ exp}$ is the individual experimentally measured *sorption capacity*; $\bar{q}_{i,exp}$ is the average of all measured experimental *sorption capacities*; n is the number of experiments performed; p is the number of model

parameters.

The R^2_{adj} and SD values were used to compare different kinetics and equilibrium models. The best-fitted model would present the R^2_{adj} closer to 1.00 and the lowest SD values (Lima et al., 2019).

2.6. Treatment of effluents

Two solutions, similar to those with a hospital origin, with different concentrations of various pharmaceuticals, organic and inorganic compounds, were prepared to test the capacity of biochar to treat real effluents (Lima et al., 2019). All absorption tests followed the same procedures as described above. Composition and concentration details are depicted in Table 1.

3. Results and discussion

3.1. Biochar characterization

3.1.1. Surface areas and porosity

Besides the chemical structure, the porosity, including SSA and micro-mesopore structures, are essential properties that play a crucial role in the performances of the sorbents in the adsorption process.

N_2 isotherm curves of the four biochars are displayed in Fig. 1. According to the IUPAC classification (Thommes et al., 2015), isotherms of the biochars exhibited a hybrid type I/IV isotherm behavior. Type I because the N_2 uptake enhances at low partial pressure due to micropore filling. Type IV is related to the mesopore contribution in the biochar samples. All the isotherms did not reach a limiting value. However, at higher partial pressures, the isotherms are closer to type IV isotherms due to the appearance of the hysteresis, which is typical of mesoporous materials. Thus, all biochars exhibit a combination of micropores and mesopores in their structure.

The biochars' isotherm curves show that the temperature and doping process did not influence the isotherms' type and shape or the final N_2 amount uptaken. Instead, slight differences are seen; for instance, the Doped-biochar-600 shows the highest N_2 adsorbed amount (187 cm^3 g^{-1}) while the Biochar-600 showed the lowest value (161 cm^3 g^{-1}); this is reflected in the SSA values and porosity structure of the biochars. Table 2 shows the SSA values, micro-mesopore areas, pore volume of the biochars.

The doping process positively influenced the SSA value (Table 2);

Table 1
Composition of the two synthetic effluents.

Pharmaceuticals	Concentration (mg L^{-1})	
	Effluent A	Effluent B
Acetylsalicylic acid	10	20
Propranolol	10	20
Amoxicillin	10	20
Captopril	10	20
Nimesulide	10	20
Diclofenac	10	20
Acetaminophen	20	40
Sugars		
Saccharose	30	50
Glucose	30	50
Organic		
Urea	10	20
Citric acid	10	20
Humic acid	10	20
Sodium dodecyl sulfate	5	10
Inorganics		
Ammonium phosphate	20	30
Ammonium chloride	20	30
Sodium sulfate	10	20
Sodium chloride	50	70
Sodium carbonate	10	20
pH	6	6

which increased from 324 to 433 m^2 g^{-1}, i.e., 33.6% higher. This result follows Yue et al. (2015), who found that N-doping helped increase biochars' surface area. The increase in the SSA can be due to the thermal decomposition products of melamine mixed with the microalgae biomass (Tian and Zhou, 2022), which start to be thermally decomposed at 345 °C, which creates new spaces and pores in the biochar structure. The increase in SSA value from non-doped to doped sample evidence that the melamine can act as a spacer. In addition, the increase in the SSA is also related to the formation of the microporosity structure in the doped biochar (Mirzaeian et al., 2019), which might be due to the introduction of other gelation nuclei in the gel solution upon the addition of melamine at a low concentration (Mirzaeian et al., 2019). Furthermore, they found out that the N-doping enhanced the number of micropores in the biochars' structure, accounting for the major of the SSA. The increased micropores might be due to the reaction between carbon atoms and NH$_3$ formed during biomass pyrolysis.

Tian et al. (2016) also reported that N-doping provoked an increase in the SSA values. They also reported that heteroatom doping could partially block the pore channels of biochars, which can potentially reduce the width of the pore leading to higher micropore contribution instead of mesopores. In addition, Hussain et al. (2020) reported nitrogen doping using carbon sheet as precursor and melamine as a dopant. The doping process increased the SSA values from 182 m^2 g^{-1} to 409 m^2 g^{-1}. They explained the increase in the SSA value due to the doping of nitrogen inducing many defects in the carbon structure. These defects are advantageous to the electron transfer by generating a more approachable surface area which, in turn, causes an increase in the adsorption performance. Moreover, thermal annealing with melamine is an effective N-doping method for improving the specific surface area and pore volume, reflected as more adsorption sites (Li et al., 2016).

These results have shown that the N-doping changed the carbon surface physical properties, which can positively influence the adsorption properties of the Doped-biochar-600.

3.1.2. SEM analysis

SEM analysis was carried out to examine the effect of the N-doping process on the biochars' surface morphology. Fig. 2 exhibits the detailed biochars' surface morphologies. Both samples showed similar structures with high roughness, irregularly covered with holes and cavities of different sizes and shapes. Thus, at first look, it seems that the doping process had no considerable effect on the biochars' morphology.

However, taking a closer look, one can observe that the doping process, to some extent, influenced the surface characteristics of the biochar. Fig. 2a (non-doped sample) shows parts with no roughness or holes/cavities/cracks (see highlighted red rectangles), while in Fig. 2b, these parts are not observed. Thus, the melamine doping yielded a carbon material with more roughness, holes, and cavities on the doped biochar surface (see red circles). In addition, the images show a significant presence of macropores and ultra-macropores. Macropores are crucial for biochars used as adsorbents to remove pollutants from waters (Soltani et al., 2020); they act as solvent passage channels, allowing the solution to be transferred from the macropores to the smaller pores (in the interior of the biochars).

Melanine, when mixed with the microalgae biomass, contributes to the volatilization process since it starts to decompose at 300 °C and hence helps to develop pore structures and increase the surface area. Moreover, melanine can act as a template, allowing for the controlled formation of pores during the carbonization process, resulting in high levels of structural ordering (observed in the SEM images).

3.1.3. Raman spectroscopy

Raman spectroscopy is considered one of the most informative methods for evaluating the structural perfection and degree of order/graphitization of bio-based carbon materials. Fig. 3 shows that the D band arises due to the broken symmetry of the hexagonal structure of the carbon atoms. Defects in the lattice cause the asymmetry, also due to the
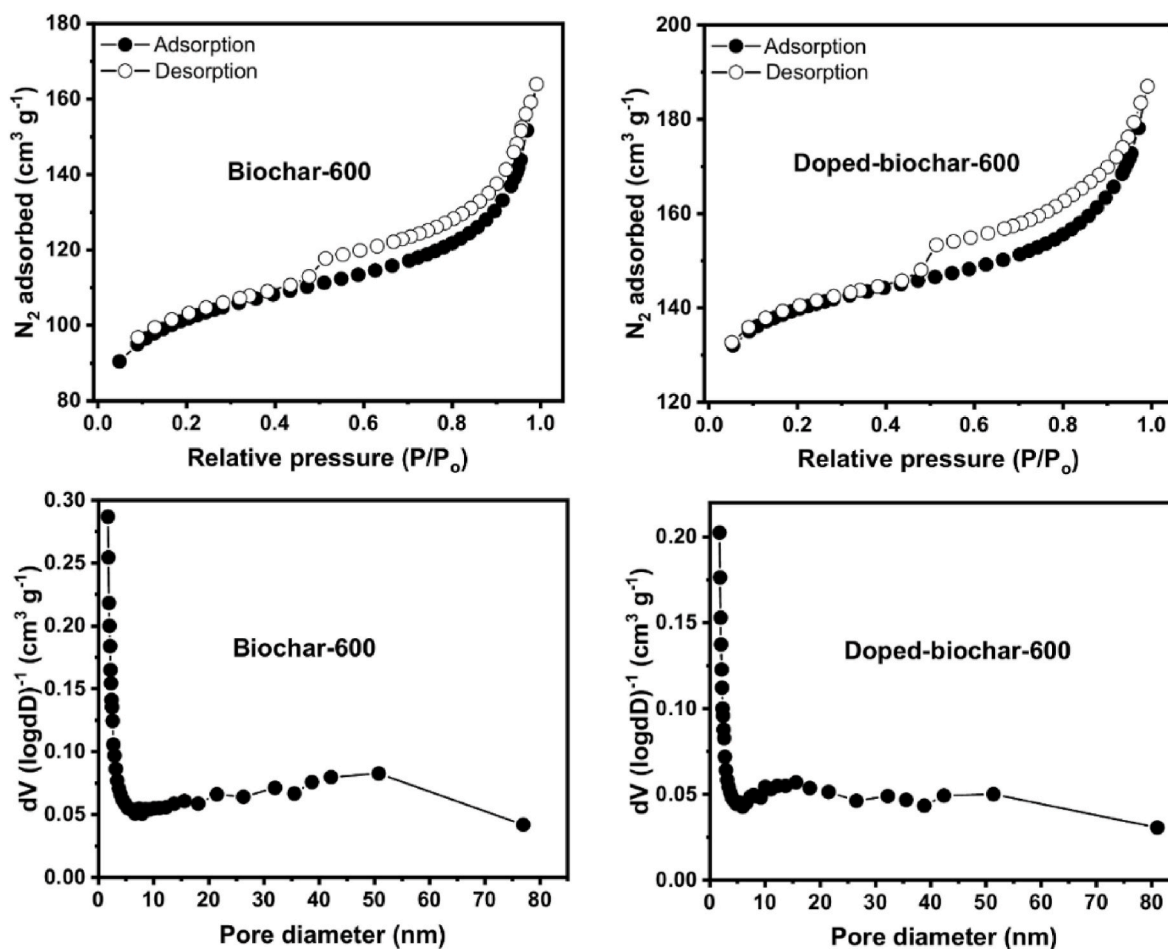
Fig. 1. N$_2$ isotherm and pore distribution curves of the biochars.

Table 2
Textural properties of the biochar samples.

Samples	SSA (m^2 g^{-1})	A$_{Micro}$ (m^2 g^{-1})	A$_{Meso}$ (m^2 g^{-1})	Pore volume (cm^3 g^{-1})
Biochar-600	324	209	115	0.25
Doped-Biochar-600	433	353	80	0.29

carbon atom sp^3 hybrid configuration, represented by a disordered and amorphous defect structure (Dos Reis et al., 2021b). The second peak at around 1600 cm^{-1} (G-peak) is characteristic of carbon atom sp^2 hybrid configuration, related to the crystalline graphite structure (Ji et al., 2021).

To further study the structural properties of the biochars, the ratio between the D and G peaks (I$_D$/I$_G$) was analyzed (values shown in Fig. 3). I$_D$/I$_G$ reveals essential information about the degree of graphitization or graphene structure and the level of perfection/order/disorder in the biochar structures (Dos Reis et al., 2021b). The I$_D$/I$_G$ decreased by
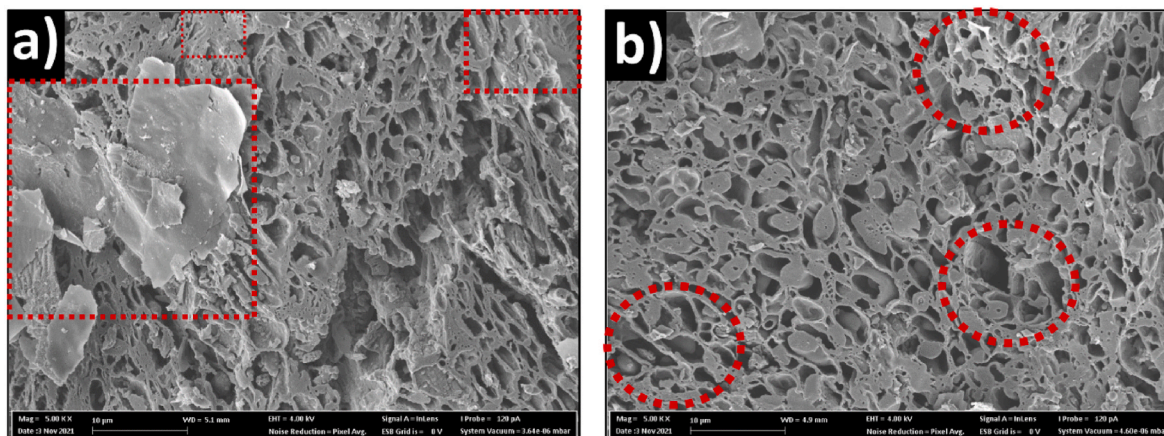

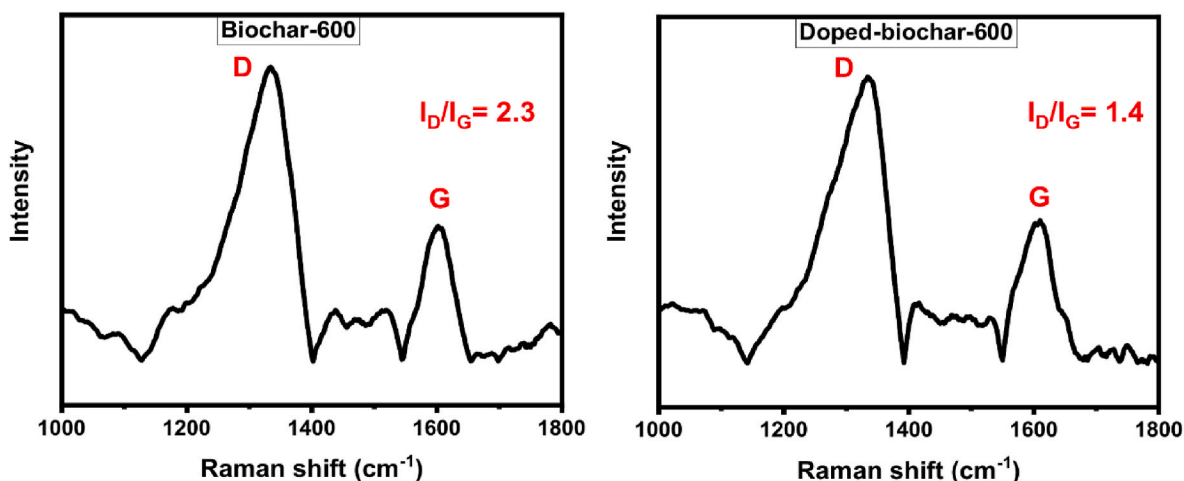**Fig. 2.** SEM images of the Biochar-600 (a) and Doped-biochar-600 (b).

Fig. 3. Raman spectra of the biochars.

doping (Fig. 3). The same behavior was reported by Ji et al. (2021) when producing nitrogen-doped porous biochar from marine algae, showing that the nitrogen doping process was responsible for reducing the I_D/I_G value (1.79) while non-doped presented an I_D/I_G of 2.19.

Although the doping process has helped decrease the I_D/I_G ratio values, both biochars have presented more defects and low graphitic structures. The lower the I_D/I_G ratio, the higher the degree of graphitization of the biochar materials. As a comparison, pure graphite has an I_D/I_G ratio of around 0.04 (Kim et al., 2013).

3.1.4. X-ray photoelectron spectroscopy

XPS analysis was performed to evaluate the biochars' functionalities and their elemental composition and chemical states. Fig. 4 shows the deconvoluted spectra for carbon (C^1s) and nitrogen (N^1s) of the four
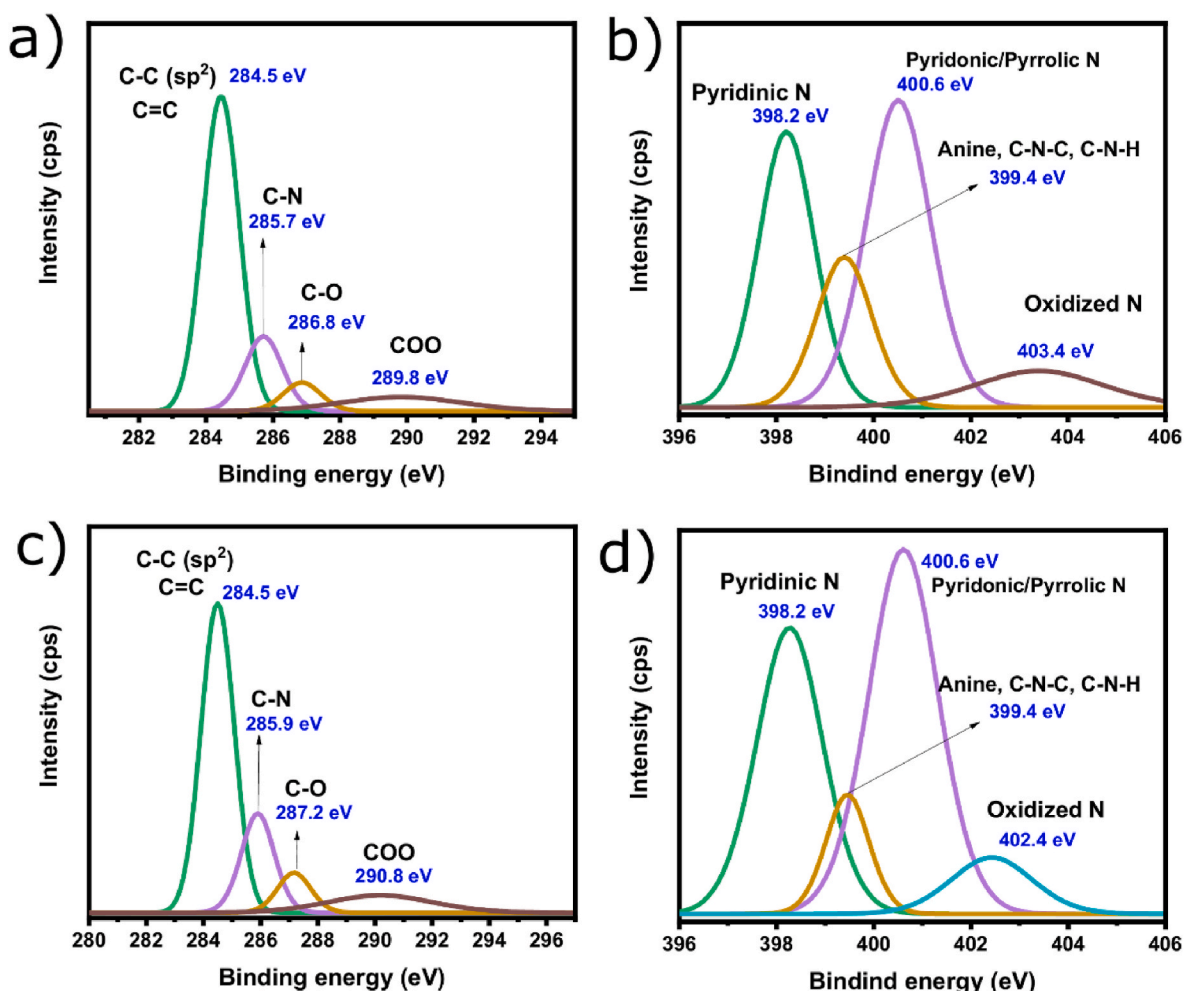

Fig. 4. XPS spectra for Biochar-600 (a,b) and Doped-biochar-600 (c,d).

biochar samples. The carbon spectrum shows four peaks for all biochars (see Fig. 4).

The deconvolution of the C1s spectrum indicates that the doped and non-doped biochars exhibit graphitic/aromatic (C=C) and hydrocarbon (C–C) at around 284.4 eV. The peak at approximately 286.5 eV is related to C–O, which is connected to ether or phenolic groups (~286.5 eV); the ester groups (O=C–O) appears at ~289.1 eV, and the carbonyl groups (C=O) is obtained at 287.5 eV (Li et al., 2020).

At first look (Fig. 4), it seems that the doping process did not influence the N species; however, Table 3, showing the quantitative information for the main elements, suggests the opposite. Here, the N content is higher in the doped biochars.

It seems that the amount of C was also influenced by the doping process which showed that C content decreased in doped sample. The XPS analysis also identified a substantial presence of oxygen, which suggests a large number of functionalities on the biochars' surfaces (Li et al., 2020). Furthermore, the doping process resulted in a sample with higher presence of N and O, which can reflect better adsorption properties (Dos Reis et al., 2021b). The higher oxygen content in the doped sample can be attributed to the physically adsorbed oxygen on the carbon surface and the oxygen atoms from N-oxide (Soo et al., 2016).

To further evaluate the effect of the doping process on nitrogen in the biochar, the N/C ratio of both samples was calculated (see Table 3) to determine their nitrogen doping level. A lower mass ratio between non-doped and doped samples indicates a higher total nitrogen content in the doped sample (0.073). To further evaluate the effect of the doping process on N's presence in the biochar structure, elemental analysis was performed, and the doped sample presented 5.3% while non-doped displayed 2.9% of N, showing that the doping process indeed inserted N in the biochar carbon matrix.

The obtained N contents are higher than some reported in the literature: Ji et al. (2021), prepared doped biochar with a nitrogen content between 1.53 and 3.47%, Lin et al. (2022), doped biochar using urea as dopant at a ratio of 1:0.5 (biomass precursor: urea) and the resulting biochar displayed 3.4% of nitrogen in its structure. However, when the ratio of dopant increased to 1:2 (biomass precursor: urea), the nitrogen content increased to 12.4%, highlighting that the amount of nitrogen in the carbon structure depends on the initial dopant amount mixed with the biomass.

Also, phosphorous (P 2p) is present in the biochars. The P is related to the H_3PO_4 activation process, which acts as the P-doping process. (Tang et al., 2021).

3.1.5. Possible doping mechanism

The nitrogen doping technique can promote many defects within the carbon material physicochemical structures. This effect is due to nitrogen acting as an electron donor that gives more electrons to the delocalized carbon network, increasing the electronic configuration of the doped carbon material, which improves the material's wettability and overall conductivity (Dos Reis et al., 2021c), which enhances the solid-liquid interface contact and, therefore, the material's adsorption properties.

When the pyrolysis takes place, the biomass precursor (mix of microalgae) and melamine start to decompose and hydrolyze, and when the temperature is further increased, it induces the carbon atoms structure rearrangement (Wang et al., 2019). Melamine decomposition

follows various stages with different intermediates. An inert product, such as C_3N_4, would be primarily generated at low temperature, and at a temperature not higher than 600 °C, the melamine starts to be incorporated to form N-dopants, i.e., pyridinic-N oxidized-N and pyrrolic-N (Wang et al., 2019); these nitrogen species were identified in the Doped-biochar-600 (see XPS results). The presence of graphitic-N is maximized at a higher temperature over 800 °C, suggesting that the organic additives would coalesce N atoms into the carbon lattice via polycondensation and co-polymerization, different from the carbon surface interaction with NH_3 molecules (Wan et al., 2020).

Fig. 5 illustrates the possible configurations of the nitrogen atoms in biochar (pyrrolic, pyridinic, graphitic, and oxidized nitrogen species). It is essential to point out that each of these species affects the electronic and transport properties of the functionalized material somewhat differently.

These results indicate that the doping process with melamine successfully generated biochar with an abundance of nitrogen species in its structure that are useful for enhancing the adsorption of acetaminophen molecules.

3.2. Adsorption results

3.2.1. Effect of the biochar mass on acetaminophen removal

In the adsorption process, the effect of the mass of the adsorbent is a fundamental step for making the adsorption process applicable on the actual industrial scale because it reduces both waste generation and costs associated with the process.

Fig. 6 shows the biochar's mass effect on the acetaminophen removal curves. It is observed that the curves behaved in the same way for both biochars. The acetaminophen percentage removal enhances as the biochar mass amount increases. On the other hand, the adsorption capacity (q) decreases with the mass increase.

The rapid increase of the acetaminophen adsorption as the biochar mass enhances is reflex of a more significant number of sorption sites are accessible to adsorb acetaminophen molecules. However, regarding q, the biochar mass increase led to a rise in the exposed area, and therefore the adsorption increases; however, because the initial acetaminophen concentration does not change and the quantity adsorbed does not increase proportionally (linearly) with the increase in biochar mass, the adsorption capacity is reduced.

Fig. 6 exhibits the effect of mass (ranging from 20 to 100 mg) on acetaminophen removal. The figure shows that the Doped-biochar-600 had the highest adsorption capacity for all studied masses among all samples. Perhaps it is because it also presented the highest SSA value, and it is well-known that the porosity and SSA have a vast influence on the adsorption process.

The most efficient biochar (Doped-biochar-600) was used to analyze the optimal biochar mass (See Fig. 6). It shows that the acetaminophen percentage of removal increased from 43.8% to 99.99% as the Doped-biochar-600 mass increased from 20 mg to 100 mg. In this work, the optimal biochar mass was 40 mg; at this mass, almost 73% of the acetaminophen was removed. When the mass increased to 60 mg (an increase of 50%), 86.1% of removal was achieved (an increase of only 13.1%). Consequently, the pH effect, kinetic, isotherm, and effluents studies were performed using 40 mg (2.0 g L^{-1}) of biochar mass.

Table 3
XPS elemental composition (atomic ratio %) and the biochars' elemental analysis (%).

Samples	XPS					N (%)[a]		N 1s state		
	C 1s	O 1s	N 1s	P 2p	N/C		N1	N2	N3	N4
Biochar-600	73.2	17.8	3.5	1.5	0.047	2.9	1.65	0.9	2.13	0.93
Doped-biochar-600	68.3	25.0	5.0	1.8	0.073	5.3	2.31	0.64	3.11	0.57

N1 = Pyridinic; N2 = Amine; N3 = Pyridonic/Pyrrolic; N4 = Oxidized.
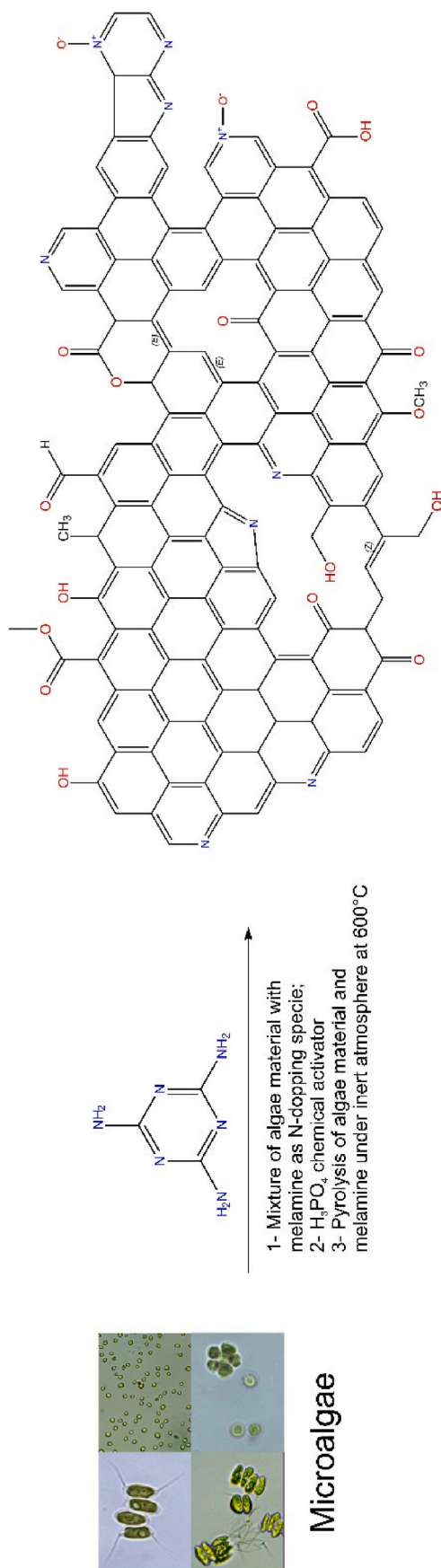
[a] Values given by elemental analysis.

Fig. 5. Schematic drawings of the different N-species formed in biochar.

1- Mixture of algae material with melamine as N-doping specie;
2- H$_3$PO$_4$ chemical activator
3- Pyrolysis of algae material and melamine under inert atmosphere at 600°C

Microalgae

3.2.2. Effect of pH of acetaminophen solution on its adsorption process

The pH of the acetaminophen solution can play an essential role due to the acetaminophen ionization and the presence of functionalities on the biochars' surface. Fig. 7 displays the acetaminophen removal percentages over the initial acetaminophen solution pH. Values of pH 2, 4, 6, 8, and 10 were tested. Within the range, the removal-% was practically constant, which indicates that the acetaminophen adsorption mechanism on non-doped and doped biochars should not be mainly due to the electrostatic interactions since it is not highly dependent on the pH values (Lima et al., 2019). This observation strengthens the idea that pore-filling should be the dominant mechanism in this adsorption process and rule out the electrostatic mechanism. Based on the pH studies, further adsorption experiments were carried out with acetaminophen solutions at pH 6.0 (deionized water).

3.2.3. Kinetic study

The kinetic is an important process for elucidating the mechanism involved in the adsorption process, such as diffusion control and mass transport processes. The kinetic process was evaluated in this work by applying three adsorption kinetic models (general order, pseudo-first-order, and pseudo-second-order). The contact time was evaluated up to 360 min at an initial 200 mg L^{-1} of acetaminophen.

Fig. 7 shows kinetic curves for the four biochars while the fitting parameters of kinetics are presented in Table 4. The curves show that at the end of 360 min, the Doped-biochar-600 adsorbed more acetaminophen (73.2 mg g^{-1}) than Biochar-600 (53.3 mg g^{-1}). The better efficiency of Doped-biochar-600 can be related to its higher SSA value and its high number of surface functionalities. It is well known that these properties are responsible for boosting the adsorption performances of adsorbents (Lima et al., 2021).

After 60 min, 89.8% and 83.2% of the acetaminophen were removed by the Biochar-600 and Doped-biochar-600 samples, respectively (Fig. 8). At 120 min, a percentage removal of 95.8 and 92.5 for the Biochar-600 and Doped-biochar-600 samples, respectively, was attained. The initial rapid adsorption could be due to the abundant active sites that easily adsorb acetaminophen molecules on the biochars' surface and pore structures. These results suggest that all biochars displayed good affinity to the acetaminophen molecules.

The suitability of the kinetic models was evaluated according to the R$^2_{adj}$ and SD values (dos Reis et al., 2020b). Lower SD and higher R$^2_{adj}$ values indicate a minor difference between experimental and theoretical q values (given by the models), and therefore, have the best suitable model. Therefore, the General order presented better fitness for all biochars based on these statistical parameters because it presented the highest R$^2_{adj}$ and lowest SD values.

The general order kinetics describes that the order of the adsorption process should be the same as that of a chemical reaction (Lima et al., 2021), while the pseudo-first-order kinetic model considers that the intraparticle mass transfer resistance plays a limiting role in adsorption. The pseudo-second-order kinetic model indicates that the adsorption mechanism plays a dominant role and is the main reason affecting adsorption (Lima et al., 2021). In a chemical reaction, the reaction order is measured experimentally (Lima et al., 2021). The general order kinetic equation presents different values for n (order of adsorption rate) when the concentration of the adsorbate is changed, making it difficult to compare the kinetic parameters of the model (Lima et al., 2021). Therefore, the initial sorption rate h$_0$ (Ho, 2006) is helpful to evaluate the kinetics of a given model, using Eq. (11):

$$h_0 = k_n \cdot q_e^n \tag{11}$$

where h$_0$ is the initial sorption rate (mg g^{-1} h^{-1}), k$_n$ is the rate constant [h^{-1} (g mg^{-1}) n^{-1}], q$_e$ is the amount adsorbed at equilibrium (mg g^{-1}), and n is the order of the kinetic model.

Considering that general order presented better fitness, more accurate h$_0$ values are obtained with this model. The values were 7.53 and
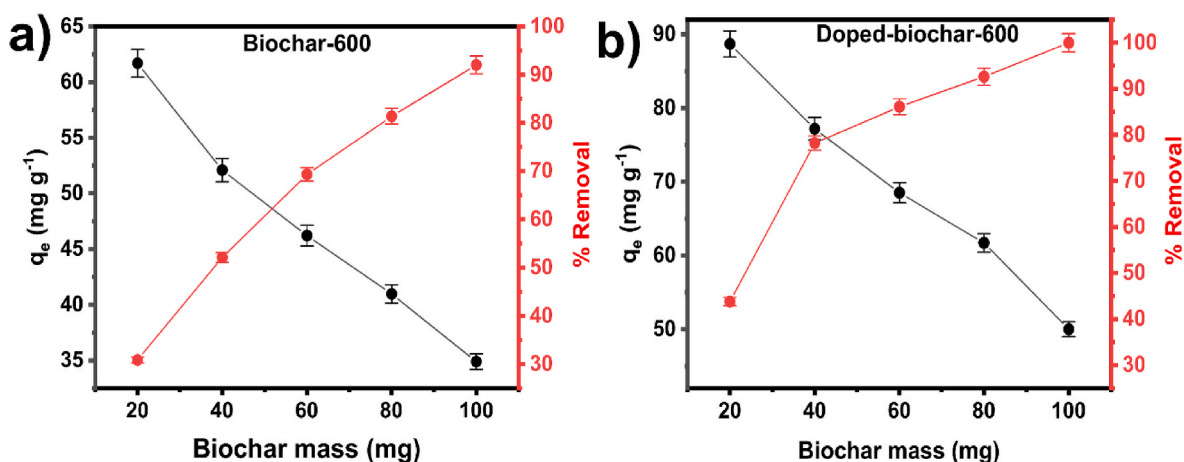
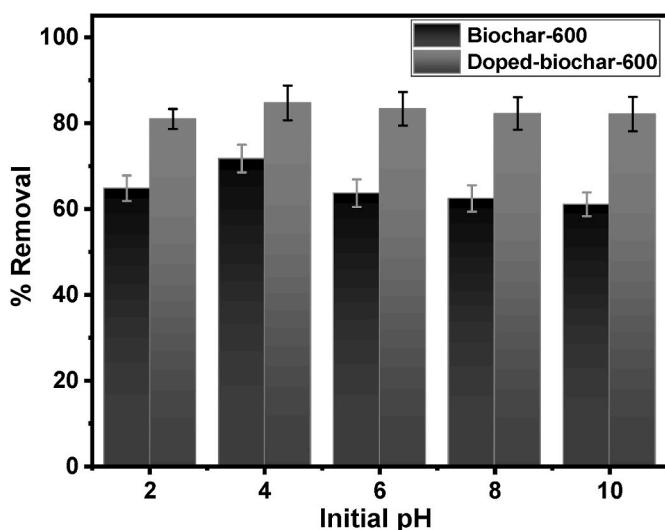**Fig. 6.** Biochar mass effect on acetaminophen adsorption.

Fig. 7. pH effect on the acetaminophen removal onto biochars at 23 °C. Adsorption experimental conditions: C_o 150 m L^{-1}, time of contact 4 h; dosage of adsorbent 2.0 g L^{-1}.

Table 4
Kinetic parameters of acetaminophen adsorption onto biochars.

Model	Biochar-600	Doped-biochar-600
Pseudo-first order		
q_1 (mg g^{-1})	48.44	62.4
k_1 (min^{-1})	0.1930	0.1301
R^2_{adj}	0.8256	0.7057
SD (mg g^{-1})	6.064	10.41
Pseudo-second order		
q_2 (mg g^{-1})	49.69	65.3
k_2 (g mg^{-1} min^{-1})	0.00921	0.00415
R^2_{adj}	0.9190	0.8376
SD (mg g^{-1})	4.130	7.734
General order		
q_n (mg g^{-1})	53.33	73.2
k_n [min^{-1} (g mg^{-1})$^{n-1}$]	0.0550	0.0456
n	1.237	1.305
h_0	7.53	12.4
R^2_{adj}	0.9837	0.9784
SD (mg g^{-1})	2.974	3.111

12.4 for Biochar-600 and Doped-biochar-600, respectively. It means that the kinetics when using the doped biochar was faster than that of non-doped biochar.

Intraparticle diffusion graphs are also shown to understand the adsorption process further (see Fig. 8c and d). The adsorption dynamics included two stages. The first stage can be related to boundary diffusion and intraparticle diffusion into the adsorbent pores; this stage is longer in the doped biochar, which may be due to the higher number of micropores that could offer more resistance to liquid penetration when compared to the mesopores. In the second stage, the acetaminophen was adsorbed and diffused into the interior site of the biochars until attaining equilibrium.

3.2.4. Equilibrium study

The adsorption equilibrium process is one of the most critical pieces of information for the correct understanding of the adsorption process (Dos Reis et al., 2021b). Moreover, it provides accurate and trustful statements about the possible mechanism of adsorption, essential for an effective design of the adsorption system.

The equilibrium system between acetaminophen and the biochars was analyzed using the nonlinear fitting of Langmuir, Freundlich, and Liu's models, and the obtained data are displayed in Fig. 9 and Table 5.

Based on that R^2_{Adj} and SD values, the Liu isotherm model was the most suitable model for all biochars because it presented the highest R^2_{Adj} and lowest SD values. Furthermore, Liu's model indicates that the adsorption process occurs on both homogeneous and heterogeneous surfaces and active sites with different energies (which is the case of our biochars) also based on multilayer adsorption. The Liu model has a hybrid adsorption mechanism, which does not follow ideal monolayer adsorption. It is a combination of the Langmuir and Freundlich isotherm models (Prola et al., 2013); therefore, the monolayer assumption of the Langmuir model is eliminated, and the infinite adsorption assumption that originates from the Freundlich model is also overruled (Lima et al., 2021). The Liu model predicts that the active sites of the adsorbent cannot have the same energy. Therefore, the biochars may have active sites preferred by the acetaminophen molecules for occupation (Lima et al., 2021); however, a saturation of the active sites should occur, unlike in the Freundlich isotherm model. Considering that the non-doped and doped biochars have different functionalities (See XPS results), it is expected that the active sites of the biochars will not have the same energy (Prola et al., 2013).

The fact that Freundlich provided a better fitness than Langmuir (see Fig. 9 and Table 5) suggests that the adsorption process of acetaminophen on both biochars was more heterogeneous than homogenous. These results agree with the biochar characterization data that showed much more defects in its structures (see Raman analysis).
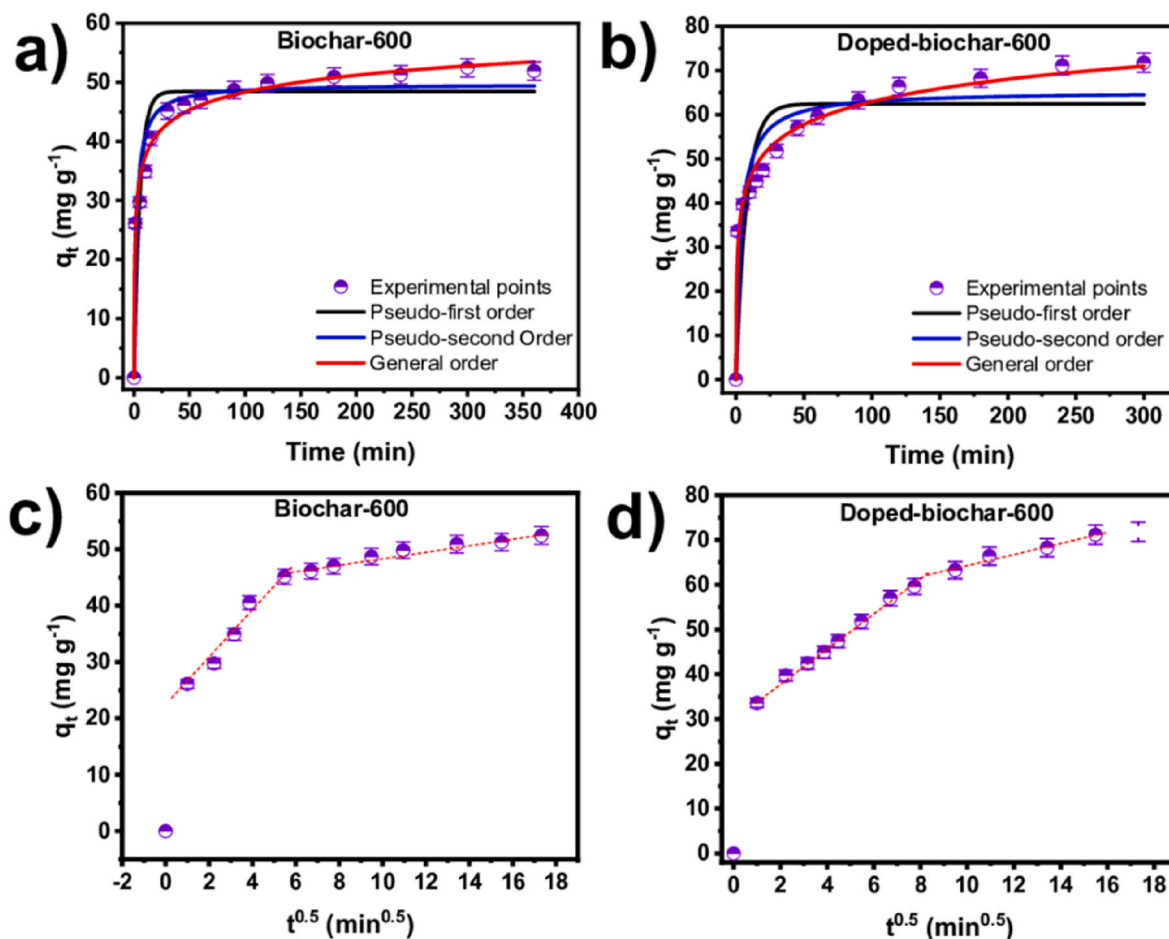
Fig. 8. Acetaminophen kinetics of adsorption curves at 23 °C onto biochars (a and b) and intraparticle curves (c and d). Conditions: Initial pH 6.0, the dosage of adsorbent 2.0 g L^{-1}.
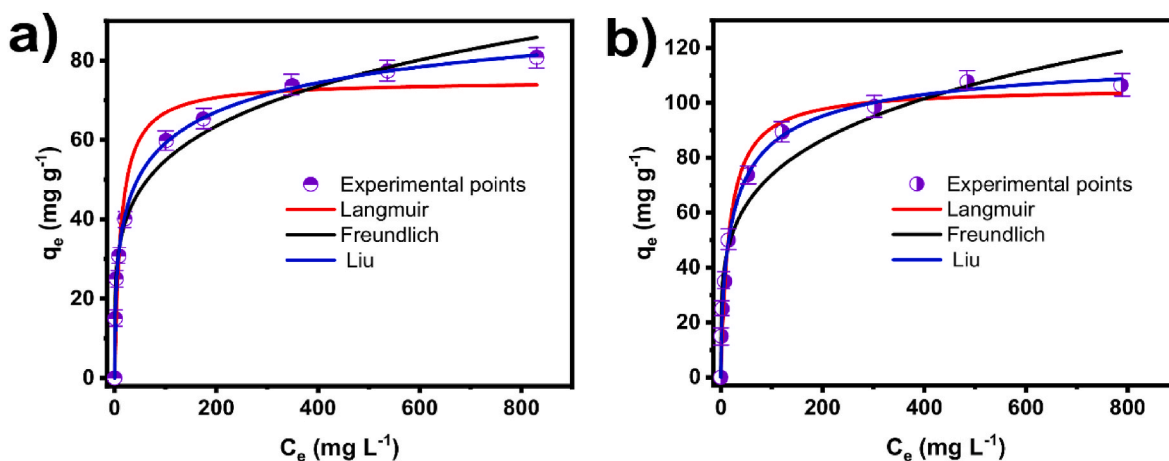

Fig. 9. Acetaminophen equilibrium curves onto Biochar-600 (a) and Doped-biochar-600 (b).

The maximum adsorption capacities for the biochars were 101.4 and 120.7 mg g^{-1} for Biochar-600 and Doped-biochar-600, respectively. The better adsorption performance of Doped-biochar-600 is related to the successful nitrogen doping process. Such doping generated biochar with improved physicochemical features, such as higher surface area and more developed surface functionality, positively affecting its adsorption performance.

The bigger SSA and amount of functionalities in doped biochar had

great significance in removing acetaminophen because the pores and functional groups help in the capillary action and the acetaminophen molecules migration into the more developed doped biochar pore structure. Moreover, the doped nitrogen on the carbon surface acts like a weak Lewis base that interacts with the oxygen-containing species through the Lewis acid-base interactions, creating many basic sites (Hussain et al., 2020), which provide delocalized electrons that boost the acetaminophen removal.

Table 5
Equilibrium parameters of acetaminophen adsorption onto biochars.

Model	Biochar-600	Doped-biochar-600
Langmuir		
Q_{Lg} (mg g^{-1})	74.92	105.6
K (min^{-1})	0.0829	0.0616
R^2_{adj}	0.9432	0.9803
SD (mg g^{-1})	6.793	5.643
Freundlich		
K_F (mg g^{-1}(mg L^{-1})$^{-1/nF}$)	20.65	25.50
n_F	4.718	4.337
R^2_{adj}	0.9837	0.9507
SD (mg g^{-1})	3.6355	8.927
Liu		
Q_{liu} (mg g^{-1})	101.4	120.7
K_{liu} (min^{-1} (g mg^{-1})$^{n-1}$)	0.01474	0.0318
n_L	0.425	0.647
R^2_{adj}	0.999	0.997
SD (mg g^{-1})	1.022	2.186

3.2.5. Acetaminophen adsorption performance over biochars and other adsorbents: comparison with literature

The adsorption tests strongly indicate that the microalgae used in this work presented satisfactory efficiency removal of acetaminophen from aqueous solutions. Although the nature of every adsorbent is different, and each absorbent has its own merits and demerits, here, we have provided comparison data with other published works. Furthermore, the values were acquired using the best-optimized conditions of each paper. As a result, it can be seen that the adsorption efficiency of the acetaminophen molecules on biochar-600 and doped-biochar-600 were very high in comparison with other listed adsorbents in Table 6.

Compared with 16 other biochars in Table 6, the Doped-biochar-600 presented one of the highest adsorption capacities, showing competitiveness in removing emerging pollutants from waters and possibly many other organic and inorganic compounds from wastewaters. Therefore, the next section is devoted to the test of the biochars in removing synthetic effluents carried with several drugs and organic and inorganic compounds commonly found in real wastewaters.

3.2.6. Synthetic wastewater treatment tests and mechanism of adsorption

As previously observed, the biochars exhibited satisfactory efficiency in removing acetaminophen from aqueous solutions. Consequently, it is expected that they can be effectively employed in the treatment of wastewaters composed of compounds commonly found in real hospitals and or pharmaceuticals wastewaters. Therefore, two synthetic wastewaters spiked with several drugs and other organic and inorganic compounds (see Table 1) were employed to test the ability of the

biochars to clean them up.

The area under the curve of UV–vis spectra of the two synthetic effluents before and after adsorption (under the band of absorption from 190 to 400 nm) was used to calculate the overall percentage removal of the compounds (Dos Reis et al., 2021a) (see Fig. 10).

The results showed high removal percentages for both biochars for both effluents, but the doped biochar exhibited a slightly better removal efficiency. Biochar-600 removed 69% and 51%, while Doped-biochar-600 removed 74% and 64% of effluent A and B, respectively. The better efficiency of nitrogen-doped biochar could be explained by its improved physicochemical characteristics, such as a well-developed porosity, higher SSA, and a higher number of surface functionalities. These results strongly support the practical application of the biochars for the removal of effluents carried with several drugs, organic and inorganic compounds.

Based on the data of characterization, pH study, kinetic and isotherm studies, and effluent treatment, it is feasible to establish the possible adsorption mechanism acting in the process (see Fig. 11).

Based on pH studies, it can be stated that electrostatic attraction was not the primary mechanism acting between acetaminophen and microalgae biochars since it was shown that the pH did not influence the acetaminophen removal. Fig. 11 highlights the contribution of the mechanism that is related to the physical-chemical interactions such as hydrogen bonding between the amide group of acetaminophen and oxygenated or nitrogenated groups of biochar, π-π interactions between the aromatic ring of the pharmaceutical and the aromatics of biochar, n-π interaction, van der Waals interactions (Thue et al., 2020). Nguyen et al. (2020) also reported a minor contribution of weak van der Waals force in the adsorption mechanism of acetaminophen on biochars.

Fig. 11 also highlights that the primary mechanism contribution for the acetaminophen removal on microalgae biochars was the pore-filling due to the well-developed pore structure and high SSA values. Furthermore, due to the dimensions of the acetaminophen molecule (1.19 nm (length), 0.75 nm (width), and 0.46 nm (thickness)), it is expectable that it can easily access micro-and mesopores present in both biochars.

4. Problems and limitations of the work

This research highlights a few problems in heteroatom-doped porous carbon adsorption of emerging pollutants. Firstly, there is rare coverage on the comparative study of adsorption capacity of the same porous carbon material modified by different heteroatoms or the different porous carbon materials doped with the same heteroatom (nitrogen), which makes it challenging to understand the influence of nitrogen and other heteroatom doping on the porous carbon material in a deeper
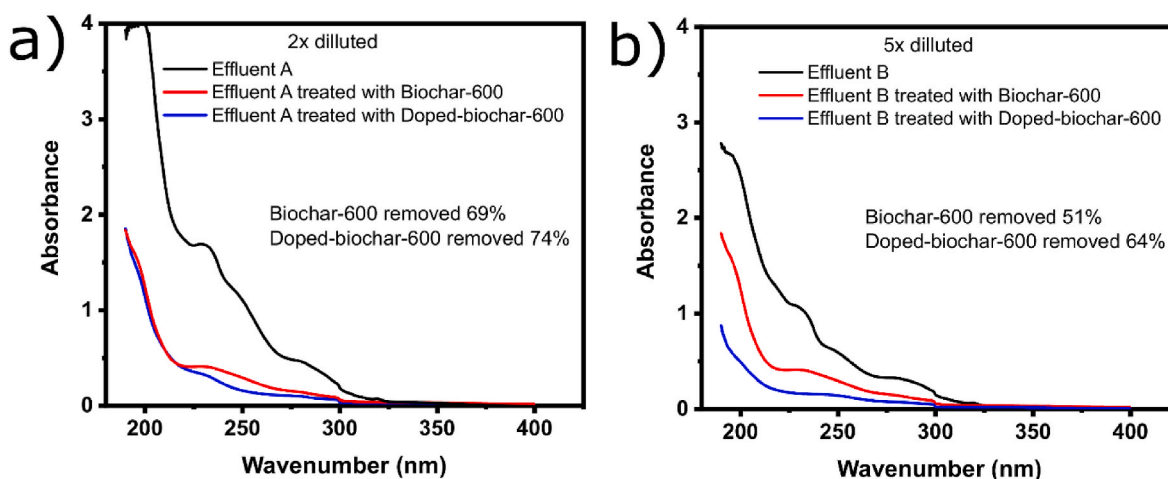
Table 6
Comparison of acetaminophen adsorption capacity and other parameters obtained from the different materials reported in the literature.

Biomass	Dosage (g L^{-1})	Activation reagent	Isotherm model	Q_{max} (mg g^{-1})	Ref.
Biochar from Kanlow Switchgrass	2.5	H$_3$PO$_4$	Langmuir	129.1	Oginni et al. (2019)
Biochar from Kanlow Switchgrass biochar	2.5	H$_3$PO$_4$	Langmuir	49.0	Oginni et al. (2019)
Biochar from Public Miscanthus	2.5	H$_3$PO$_4$	Langmuir	156.2	Oginni et al. (2019)
Biochar from Public Miscanthus biochar	2.5	H$_3$PO$_4$	Langmuir	14.0	Oginni et al. (2019)
Biochar from Cashew nutshell	0.5	H$_3$PO$_4$	Langmuir	90	Geczo et al., 2021
Biochar from Cashew nutshell	0.5	H$_3$PO$_4$	Langmuir	77	Geczo et al., 2021
Biochar from Cashew nutshell	0.5	H$_3$PO$_4$	Langmuir	146	Geczo et al., 2021
Biochar from Cashew nutshell	0.5	H$_3$PO$_4$	Langmuir	132	Geczo et al., 2021
Amine functionalized superparamagnetic silica nanocomposite	–	–	Langmuir	58	Kollarahithlu and Balakrishnan (2021)
Rhamnolipid based chitosan magnetic nanosorbents	4.0	–	Langmuir	96.35	Natarajan et al., 2022
Nanocomposite polymers	1.0	–	Langmuir	71.9	Mphahlele et al. (2015)
Nanocomposite polymers	1.0	–	Langmuir	41.0	Mphahlele et al. (2015)
Biochar from cork powder	–	K$_2$CO$_3$	Langmuir	200	Spessato et al. (2019)
Biochar from jatobá	1.0	KOH	Langmuir	300	Cabrita et al. (2010)
Biochar-600	2.0	H$_3$PO$_4$	Liu	101.4	This work
Doped-biochar-600	2.0	H$_3$PO$_4$	Liu	120.7	This work

Fig. 10. Adsorption of synthetic effluent. Effluent A (a); Effluent B (b). See Table 1 for the composition of effluents.

level.

Secondly, the solutions used in these studies are almost concocted in the laboratory, significantly different from the real wastewaters. These studies are carried out under laboratory conditions, which are too idealistic to apply at an industrial scale, and industrial factors should be more considered in future research. Given the above problems, some challenges and future studies are stated as in the following section:

5. Conclusion

This work show results from a new type of N-doped porous activated biochar developed from a wild mixture of microalgae grown in a pilot-scale municipal wastewater treatment plant. Adsorbents were developed using H_3PO_4 as activation agent and melanine as N-rich dopant agent. The activation procedure was carried out using a one-step preparation/activation method. The biochars were tested for their performance during the removal of acetaminophen from water and contaminants from synthetic effluents. The main results from this research showed that:

- The specific results of this research showed that the doping process led to an increase in the SSA by 33.6% compared to the non-doped sample. In addition, the doping process generated biochar with a much higher number of micropores, which are both favorable diffusion channels for emerging pollutants' internal diffusion and boost its adsorption performance.
- The doping process positively helped increase the graphitization degree in the biochar and increase the amount of oxygen and nitrogen groups on the biochar's surface, which further boosts its adsorption performances through electrostatic attractions.
- The biochars were successfully employed to adsorbed acetaminophen and other compounds from synhetic effluents. It was found that the N-doped biochar presented the highest efficiency.
- The primary mechanism of adsorption for the acetaminophen on the microalgal biochars was pore-filling.
- The employment of the biochars in the treatment of synthetic effluents, containing several other emerging pollutants, showed a very satisfactory percentage of removal (up to 74%).

The above results strongly suggest that the microalgae consortium used in this work can be considered a high-efficiency precursor for biochar preparation, effectively treating polluted waters.

6. Challenges and future works

(i) Difficulties in controlling and understanding the pore geometry and pore size in chemical activators and nitrogen doping processes to obtain carbon materials with high specific surface area and hierarchical porous structure.

(ii) Insufficient fundamental understanding of the mechanisms and effects of nitrogen doping methods on the surface area, pore size, and surface chemistry connected to the biomass-derived carbon materials adsorption performances.

(iii) Difficulties in selecting suitable biomass materials to obtain effective heteroatom(s)-doping to increase interlayer spacing, defects, and active sites because not all heteroatom(s)-doping can play active roles in the enhancement of adsorption properties. There is a need to tailor the doped carbon material based on heteroatom doping (e.g., nitrogen) to target the removal of specific contaminant (s).

(iv) Insufficient understanding of the performance enhancement mechanisms of incorporating suitable heteroatom (N, O, S, H, P) into biomass-derived carbon materials. Furthermore, because synergetic effects between carbon networks and heteroatoms can enhance adsorption performance, the generation of synergistic effects and the understanding of their functional mechanisms need to be further examined.

(v) The other selection of suitable biomass sources and the development/optimization of corresponding cost-effective synthesis methods to achieve high-performance biomass-derived carbon materials and their doped ones. Here, doping carbon materials with other elements such as N, S, O, and P are effective methods to create synergetic effects and enhance material performance in environmental and other applications.

(vi) The exploration of possible opportunities for not only microalgae carbon materials but any kind of biomass-derived carbon materials and their respective doped ones to obtain sustainable, versatile, and efficient carbon materials for environmental and a wide range of other applications.

CRediT authorship contribution statement

María González-Hourcade: Investigation, Methodology, Writing – original draft. **Glaydson Simões dos Reis:** Writing – original draft, Conceptualization, Software, Data curation, Supervision. **Alejandro Grimm:** Investigation, Methodology, Writing – review & editing. **Van Minh Dinh:** Software, Data curation. **Eder Claudio Lima:** Software, Data curation, Writing – review & editing. **Sylvia H. Larsson:** Writing – review & editing, Funding acquisition. **Francesco G. Gentili:** Writing –
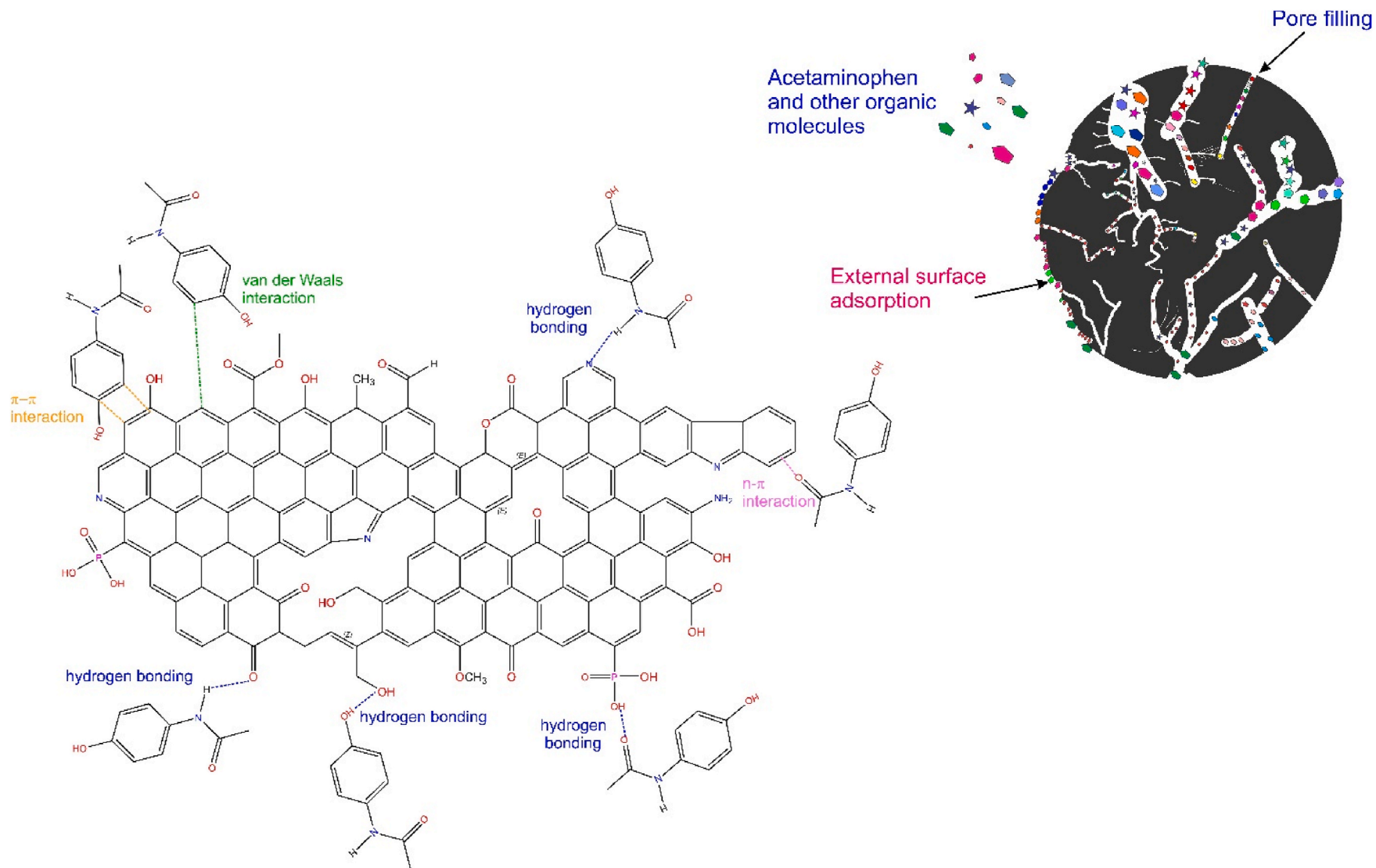
Fig. 11. Proposed adsorption mechanism for uptake of acetaminophen onto biochars.

review & editing, Supervision, Funding acquisition.

Declaration of competing interest

The authors declare that they have no known competing financial interests or personal relationships that could have appeared to influence the work reported in this paper.

Acknowledgements

References

Bădescu, I.S., Bulgariu, D., Ahmad, I., Bulgariu, L., 2018. Valorisation possibilities of exhausted biosorbents loaded with metal ions – a review. J. Environ. Manag. 224, 288–297. https://doi.org/10.1016/j.jenvman.2018.07.066.

Boumya, W., Taoufik, N., Achak, M., Barka, N., 2021. Chemically modified carbon-based electrodes for the determination of paracetamol in drugs and biological samples. J. Pharm. Anal. 11, 138–154. https://doi.org/10.1016/j.jpha.2020.11.003.

Cabrita, I., Ruiz, B., Mestre, A.S., Fonseca, I.M., Carvalho, A.P., Ania, C.O., 2010. Removal of an analgesic using activated carbons prepared from urban and industrial residues. Chem. Eng. J. 163, 249–255. https://doi.org/10.1016/j.cej.2010.07.058.

Daughton, C.G., 2014. The Matthew effect and widely prescribed pharmaceuticals lacking environmental monitoring: a case study of an exposure-assessment vulnerability. Sci. Total Environ. 466, 315–325. https://doi.org/10.1016/j.scitotenv.2013.06.111.

Dharupaneedi, S.P., Nataraj, S.K., Nadagouda, M.P., Reddy, K.R., Shukla, S.S., Aminabhavi, T.M., 2019. Membrane-based separation of potential emerging pollutants. Separ. Purif. Technol. 210, 850–866. https://doi.org/10.1016/j.seppur.2018.09.003.

Dos Reis, G.S., Adebayo, M.A., Lima, E.C., Sampaio, C.H., Prola, L.D.T., 2016. Activated carbon from sewage sludge for preconcentration of copper. Anal. Lett. 49, 541–555. https://doi.org/10.1080/00032719.2015.1076833.

Dos Reis, G.S., Larsson, S.H., Mathieu, M., Thyrel, M., Tung, P., 2021a. Application of Design of Experiments (DoE) for Optimised Production of Micro-and Mesoporous Norway Spruce Bark Activated Carbons. Biomass Conv. Bioref. https://doi.org/10.1007/s13399-021-01917-9.

Dos Reis, G.S., Larsson, S.H., Thyrel, M., Pham, T.N., Lima, E.C., de Oliveira, H.P., Dotto, G.L., 2021b. Preparation and application of efficient biobased carbon adsorbents prepared from spruce bark residues for efficient removal of reactive dyes and colors from synthetic effluents. Coatings 11, 772. https://doi.org/10.3390/coatings11070772.

Dos Reis, G.S., Oliveira, H.P.d., Larsson, S.H., Thyrel, M., Lima, E.C., 2021c. A short review on the electrochemical performance of hierarchical and nitrogen-doped activated biocarbon-based electrodes for supercapacitors. Nanomaterials 11, 424. https://doi.org/10.3390/nano11020424.

Fast, S.A., Gude, V.G., Truax, D.D., Matin, J., Magbanua, B.J., 2017. A critical evaluation of advanced oxidation processes for emerging contaminants removal. Environ. Process. 4, 283–302. https://doi.org/10.1007/s40710-017-0207-1.

Geczo, A., Giannakoudakis, D.A., Triantafyllidis, K., Ragab Elshaer, M., Rodríguez-Aguado, E., Bashkova, S., 2021. Mechanistic insights into acetaminophen removal on cashew nutshell biomass-derived activated carbons. Environ. Sci. Pollut. Res. 28, 58969–58982. https://doi.org/10.1007/s11356-019-07562-0.

Guo, Q., Bandala, E.R., Goonetilleke, A., Hong, N., Li, Y., Liu, A., 2021. Application of *Chlorella pyrenoidosa* embedded biochar beads for water treatment. J. Water Proc. Eng. 40, 101892. https://doi.org/10.1016/j.jwpe.2020.101892.

Ho, Y.S., 2006. Review of second-order models for adsorption systems. J. Hazard Mater. 136, 681–689. https://doi.org/10.1016/j.jhazmat.2005.12.043.

Hussain, I., Qi, J., Sun, X., Wang, L., Li, J., 2020. Melamine derived nitrogen-doped carbon sheet for the efficient removal of chromium (VI). J. Mol. Liq. 318, 114052. https://doi.org/10.1016/j.molliq.2020.114052.

Ilnicka, A., Lukaszewicz, J.P., 2018. Marine and freshwater feedstocks as a precursor for nitrogen-containing carbons: a review. Mar. Drugs 16, 142. https://doi.org/10.3390/md16050142.

Ji, R., Wu, Y., Bian, Y., Song, Y., Sun, Q., Jiang, X., Zhang, L., Han, J., Cheng, H., 2021. Nitrogen-doped porous biochar derived from marine algae for efficient solid-phase microextraction of chlorobenzenes from aqueous solution. J. Hazard Mater. 407, 124785. https://doi.org/10.1016/j.jhazmat.2020.124785.

Kanaujiya, D.K., Paul, T., Sinharoy, A., Pakshirajan, K., 2019. Biological treatment processes for the removal of organic micropollutants from wastewater: a review. Curr. Pollut. Rep. 5, 112–128. https://doi.org/10.1007/s40726-019-00110-x.

Kasperiski, F.M., Lima, E.C., Umpierres, C.S., dos Reis, G.S., Thue, P.S., Lima, D.R., Dias, S.L.P., Saucier, C., da Costa, J.B., 2018. Production of porous activated carbons from *Caesalpinia ferrea* seed pod wastes: highly efficient removal of captopril from aqueous solutions. J. Clean. Prod. 197, 919–929. https://doi.org/10.1016/j.jclepro.2018.06.146.

Kim, S.-G., Park, O.-K., Lee, J.-H., Ku, B.-C., 2013. Layer-by-layer assembled graphene oxide films and barrier properties of thermally reduced graphene oxide membranes. Carbon Letters 14, 247–250. https://doi.org/10.5714/CL.2013.14.4.247.

Klotz, U., 2012. Paracetamol (acetaminophen) – a popular and widely used nonopioid analgesic. Arzneimittelforschung 62, 355–359. https://doi.org/10.1055/s-0032-1321785.

Ko, D.C.K., Mui, E.L.K, Lau, K.S.T., McKay, G., 2004. Production of activated carbons from the waste tire – process design and economic analysis. Waste Manag. 24, 875–888. https://doi.org/10.1016/j.wasman.2004.03.006.

Kollarahithlu, S.C., Balakrishnan, R.M., 2021. Adsorption of pharmaceuticals pollutants, Ibuprofen, Acetaminophen, and Streptomycin from the aqueous phase using amine-functionalized superparamagnetic silica nanocomposite. J. Clean. Prod. 294, 126155. https://doi.org/10.1016/j.jclepro.2021.126155.

Kroon, F.J., Berry, K.L.E., Brinkman, D.L., Kookana, R., Leusch, F.D.L., Melvin, S.D., Neale, P.A., Negri, A.P., Puotinen, M., Tsang, J.J., van de Merwe, J.P., Williams, M., 2020. Sources, presence, and potential effects of contaminants of emerging concern in the marine environments of the Great Barrier Reef and Torres Strait, Australia. Sci. Total Environ. 719, 135140. https://doi.org/10.1016/j.scitotenv.2019.135140.

Lage, S., Toffolo, A., Gentili, F.G., 2021. Microalgal growth, nitrogen uptake and storage, and dissolved oxygen production in a polyculture based-open pond fed with municipal wastewater in northern Sweden. Chemosphere 276, 130122. https://doi.org/10.1016/j.chemosphere.2021.130122.

Lewoyehu, M., 2021. Comprehensive review on synthesis and application of activated carbon from agricultural residues for the remediation of venomous pollutants in wastewater. J. Anal. Appl. Pyrol. 159, 105279. https://doi.org/10.1016/j.jaap.2021.105279.

Li, Y., Hussain, I., Qi, J., Liu, C., Li, J., Shen, J., Sun, X., Han, W., Wang, L., 2016. N-doped hierarchical porous carbon derived from hypercrosslinked diblock copolymer for capacitive deionization. Separ. Purif. Technol. 165, 190–198. https://doi.org/10.1016/j.seppur.2016.04.007.

Li, J., He, F., Shen, X., Hu, D., Huang, Q., 2020. Pyrolyzed fabrication of N/P co-doped biochars from (NH4)3PO4-pretreated coffee shells and appraisement for remedying aqueous Cr (VI) contaminants. Biores.Tech. 315, 123840. https://doi.org/10.1016/j.biortech.2020.123840.

Lima, D.R., Bandegharaei, A.H., Thue, P.S., Lima, E.C., de Albuquerque, Y.R.T., dos Reis, G.S., Umpierres, C.S., Dias, S.L.P., Tran, H.N., 2019. Efficient acetaminophen removal from water and hospital effluents treatment by activated carbons derived from Brazil nutshells. Colloids Surf., A 583, 123966. https://doi.org/10.1016/j.colsurfa.2019.123966.

Lima, E.C., Dehghani, M.H., Guleria, A., Sher, F., Karri, R.R., Dotto, G.L., Tran, H.N., 2021. Chapter 3 - adsorption: Fundamental aspects and applications of adsorption for effluent treatment. In: Hadi Dehghani, M., Karri, R., Lima, E. (Eds.), Green Technologies for the Defluoridation of Water. Elsevier, pp. 41–88.

Lin, S., Yang, X., Liu, L., Li, A., Qiu, G., 2022. Electrosorption of cadmium and arsenic from wastewaters using nitrogen-doped biochar: mechanism and application. J. Environ. Manag. 301, 113921. https://doi.org/10.1016/j.jenvman.2021.113921.

Mahima, J., Sundaresh, R.K., Gopinath, K.P., Rajan, P.S.S., Arun, J., Kim, S.-H., Pugazhendhi, A., 2021. Effect of algae (*Scenedesmus obliquus*) biomass pre-treatment on bio-oil production in hydrothermal liquefation (HTL): biochar and aqueous phase utilization studies. Sci. Total Environ 778, 146262. https://10.1016/j.scitotenv.2021.1462.

Masoumi, S., Dalai, A., 2020. Optimized production and characterization of highly porous activated carbon from algal-derived hydrochar. J. Clean. Prod. 263, 121427. https://doi.org/10.1016/j.jclepro.2020.121427.

Mirzaeian, M., Abbas, Q., Gibson, D., Mazur, M., 2019. Effect of nitrogen doping on the electrochemical performance of resorcinol-formaldehyde based carbon aerogels as electrode material for supercapacitor applications. Energy 173, 809–819.

Mohsenpour, S.F., Hennige, S., Willoughby, N., Adeloye, A., Gutierrez, T., 2021. Integrating micro-algae into wastewater treatment: a review. Sci. Total Environ. 752 (15), 142168. https://doi.org/10.1016/j.scitotenv.2020.142168.

Mphahlele, K., Onyango, M.S., Mhlang, S.D., 2015. Adsorption of aspirin and paracetamol from aqueous solution using Fe/N-CNT/b-cyclodextrin nanocomposites synthesized via a benign microwave-assisted method. J. Environ. Chem. Eng. 3, 2619–2630. https://doi.org/10.1016/j.jece.2015.02.018.

Naeem, M.A., Imran, M., Amjad, M., Abbas, G., Tahir, M., Murtaza, B., Zakir, A., Shahid, M., Bulgariu, L., Ahmad, I., 2019. Batch and column scale removal of cadmium from water using raw and acid activated wheat straw biochar. Water 11, 1438. https://doi.org/10.3390/w11071438.

Natarajan, R., Kumar, M.N., Vaidyanathan, V.K., 2022. Synthesis and characterization of rhamnolipid based chitosan magnetic nano sorbent for the removal of acetaminophen from aqueous solution. Chemosphere 288, 132532. https://doi.org/10.1016/j.chemosphere.2021.132532.

Nguyen, D.T., Tran, H.N., Juang, R.S., Dat, N.D., Tomul, F., Ivanets, A., Woo, S.H., Hosseini-Bandegharaei, A., Nguyen, V.P., Chao, H.P., 2020. Adsorption process and mechanism of acetaminophen onto commercial activated carbon. J. Environ. Chem. Eng. 8, 104408. https://doi.org/10.1016/j.jece.2020.104408.

Oginni, O., Singh, K., Oporto, G., Dawson-Andoh, B., McDonald, L., Sabolsky, E., 2019. Effect of one-step and two-step H3PO4 activation on activated carbon

characteristics. Bioresour. Technol. Rep. 8, 100307. https://doi.org/10.1016/j.biteb.2019.100307.

Prola, L.D.T., Acayanka, E., Lima, E.C., Umpierres, C.S., Vaghetti, J.C.P., Santos, W.O., Laminsi, S., Djifon, P.T., 2013. Comparison of Jatropha curcas shells in natural form and treated by non-thermal plasma as biosorbents for removal of Reactive Red 120 textile dye from aqueous solution. Ind. Crop. Prod. 46, 328–340. https://doi.org/10.1016/j.indcrop.2013.02.018.

Soltani, R., Marjani, A., Soltani, R., Shirazian, S., 2020. Hierarchical multi-shell hollow micro–meso–macroporous silica for Cr(VI) adsorption. Sci. Rep. 10, 9788. https://doi.org/10.1038/s41598-020-66540-6.

Soo, L.T., Loh, K.S., Mohamad, A.B., Daud, W.R.W., Wong, W.Y., 2016. Effect of nitrogen precursors on the electrochemical performance of nitrogen-doped reduced graphene oxide towards oxygen reduction reaction. J. Alloys Compd. 677, 112–120.

Spessato, L., Bedin, L.C., Cazetta, A.L., Souza, I.P.A.F., Duarte, V.A., Crespo, L.H.S., Silva, M.C., Pontes, R.M., Almeida, V.C., 2019. KOH-super activated carbon from biomass waste: insights into the paracetamol adsorption mechanism and thermal regeneration cycles. J. Hazard Mater. 371, 499–505. https://doi.org/10.1016/j.jhazmat.2019.02.102.

Tang, W., Zanli, B.L.G.L., Chen, J., 2021. O/N/P-doped biochar induced to enhance adsorption of sulfonamide with coexisting Cu2+/Cr (VI) by air pre-oxidation. Bioresour. Technol. 341, 125794. https://doi.org/10.1016/j.biortech.2021.125794.

Thommes, M., Kaneko, K., Neimark, A.V., Olivier, J.P., Rodriguez-Reinoso, F., Rouquerol, J., 2015. Physisorption of gases, with special reference to the evaluation of surface area and pore size distribution (IUPAC technical report). Pure Appl. Chem. 87, 1051–1069. https://doi.org/10.1515/pac-2014-1117.

Thue, P.S., Umpierres, C.S., Lima, E.C., Lima, D.R., Machado, F.M., Reis, G.S., Silva, R.S., Pavan, F.A., Tran, H.N., 2020. Single-step pyrolysis for producing magnetic activated carbon from tucumã (Astrocaryum aculeatum) seed and nickel (II) chloride and zinc (II) chloride. Application for removal of nicotinamide and propranolol. J. Hazard Mater. 398, 122903. https://doi.org/10.1016/j.jhazmat.2020.122903, 2020.

Tian, Y., Zhou, H., 2022. A novel nitrogen-doped porous carbon derived from black liquor for efficient removal of Cr(VI) and tetracycline: comparison with porous lignin carbon. J. Clean. Prod. 333, 130106.

Tian, W., Zhang, H., Duan, X., Sun, H., Tade, M.O., Ang, H.M., Wang, S., 2016. Nitrogen- and sulfur-codoped hierarchically porous carbon for adsorptive and oxidative removal of pharmaceutical contaminants. ACS Appl. Mater. Interfaces 8, 7184–7193. https://doi.org/10.1021/acsami.6b01748.

Umpierres, C.S., Thue, P.S., dos Reis, G.S., de Brum, I.A.S., Lima, E.C., de Alencar, W.A., Dias, S.L.P., Dotto, G.L., 2018. Microwave activated carbons from Tucumã (Astrocaryum aculeatum) waste for efficient removal of 2-nitrophenol from aqueous solutions. Environ. Technol. 39, 173–1187. https://doi.org/10.1080/09593330.2017.1323957.

Von der Ohe, P.C., Dulio, V., Slobodnik, J., De Deckere, E., Kühne, R., Ebert, R.-U., 2011. A new risk assessment approach for the prioritization of 500 classical and emerging organic microcontaminants as potential river basin specific pollutants under the European Water Framework Directive. Sci. Total Environ. 409, 2064–2077. https://doi.org/10.1016/j.scitotenv.2011.01.054.

Wan, Z., Sun, Y., Tsang, D.C.W., Khan, E., Yip, A.C.K., Ng, Y.H., Rinklebe, J., Ok, Y.S., 2020. Customised fabrication of nitrogen-doped biochar for environmental and energy applications. Chem. Eng. J. 401, 126136. https://doi.org/10.1016/j.cej.2020.126136.

Wang, Y., Chen, W., Chen, C., Xi, J., Cao, H., Duan, X., Xie, Y., Song, W., Wang, S., 2019. Occurrence of both hydroxyl radical and surface oxidation pathways in N-doped layered nanocarbons for aqueous catalytic ozonation. Appl. Catal., B 254, 283–291. https://doi.org/10.1016/j.apcatb.2019.05.008.

Xu, L., Wu, C., Chai, C., Cao, S., Bai, X., Ma, K., Jin, X., Shi, X., Jin, P., 2022. Adsorption of micropollutants from wastewater using iron and nitrogen co-doped biochar: performance, kinetics and mechanism studies. J. Hazard Mater. 424, 127606. https://doi.org/10.1016/j.jhazmat.2021.127606.

Yaashikaa, P.R., Kumar, P.S., Varjani, S., Saravanan, A., 2020. A critical review on the biochar production techniques, characterization, stability and applications for circular bioeconomy. Biotechnol. Rep. 28, e00570 https://doi.org/10.1016/j.btre.2020.e00570.

Yue, G., Meng, K., Liu, Q., 2015. One-step synthesis of n-doped carbon and its application as a cost-efficient catalyst for the oxygen reduction reaction in microbial fuel cells. ChemPlusChem 80, 1133–1138. https://doi.org/10.1002/cplu.201500057.